ELSEVIER

Journal of Alloys and Compounds 323–324 (2001) 34–38

Journal of ALLOYS AND COMPOUNDS

www.elsevier.com/locate/jallcom

Chemical inhomogeneity in materials with f-elements: observation and interpretation

I.G. Vasilyeva*

Institute of Inorganic Chemistry, Russian Academy of Sciences, Siberian Branch, Lavrentiev Avenue 3, 630090 Novosibirsk, Russia

Abstract

Novel possibility to control local chemical inhomogeneities, acting on functional properties of materials, appeared due to the differential dissolution (DD) technique. A series of materials, such as thin films ZnS·EuS/Si and $YBa_2Cu_3O_x$/sapphire, crystals $TmBa_2Cu_3O_x$·CaO, powders γ-Ce_2S_3·Na_2S and $LaFeO_3$·CaO have been analyzed and the DD patterns with different profiles of kinetic curves of elements dissolving and stoichiograms were collected. The origin of the local inhomogeneities was established by analysis of these profiles. The inhomogeneity manifested itself as separate phases, as spatial compositional nonuniformity of solid solutions, as the grain surface enriched by doping elements, as non-stoichiometry produced by undesired doping with the container or substrate elements. In all cases, the DD results were compared with those obtained by other assessment techniques.

Keywords: Materials with f-elements; Chemical inhomogeneity; Differential dissolving analysis

1. Introduction

The development in the field of materials science tends toward improved quality of materials especially their chemical homogeneity. The term chemical inhomogeneity is used in reference to any local compositional feature associated with the presence of separate phases, spatial compositional nonuniformity of solid solutions, a composition variation through incorporation of undesired elements. Given the small dimensions of these features one needs an analytical technique with high spatial and depth resolution, as for instance the known analytical electron microscopy, scanning Auger electron spectroscopy, angle-resolved X-ray photoelectron spectroscopy. The objective of this paper is to show the potential of other technique, DD, which taken alone or in combination with scanning electron microscopy (SEM) may also observe and quantitatively estimate the scale of the chemical inhomogeneity. The use of the DD is illustrated here by examples with different materials useful for applications. The DD technique somewhat resembles the destructive Auger depth profiling method [1]. However, contrary to the latter, DD has no need of ultrahigh vacuum, does not suffer from any artifacts and has no problem with charging and topographic effects of samples. Besides, DD having depth resolution as 30 Å cm^{-2}, detection sensitivity as 30–100 ppb and error as 3% is a truly selective method and interpretation of depth profiles in the context of phase identification has no need of the phase standard references [2]. As regards materials under study, they all were on way to optimized quality and, therefore, excellent to demonstrate comprehensively of the DD power.

2. Experimental

To illustrate the DD power independent from shape or dimension of samples three types of materials were analyzed: powders, Ce_2S_3·Na_2S and $LaFeO_3$·CaO; thin films ZnS·EuS/Si and $YBa_2Cu_3O_x$/sapphire; crystals $TmBa_2Cu_3O_x$·CaO. To show DD as a precise, sensitive and proximate method, multi-element systems with high chance to be heterophased have been examined. To assure various types of inhomogeneity the samples prepared differently were analyzed. This was MO-CVD for Zn–Eu–S [3], laser ablation for Y–BaCu–O [4], crystallization from melt for Tm–Ca–Ba–Cu–O, high temperature solid–gas and solid–solid reactions for Ce–Na–S [5] and La–Ca–Fe–O [6].

DD measurements are performed with a suitable solvents, HNO_3 acid, which concentration are forced increas-

*Fax: +7-3832-344-489.

E-mail address: kamarz@che.nsk.su (I.G. Vasilyeva).

0925-8388/01/$ – see front matter
PII: S0925-8388(01)01003-9

ing from 0.01 to 0.1 M and HCl with that from 0 to 0.1 M. The solvent passes over a sample with a constant velocity and the solution formed is directed to analyzer, ICP AES, where concentration of all elements composing the sample is determined continuously. Usually 150–300 compositional points are determined to record the kinetic curves of elements dissolving and stoichiograms, i.e. molar ratios of these elements. This was possible even for a sample with weight of several micrograms. The kinetic data obtained for elements are recalculated into these for phases due to special computer programs. In this paper, all the DD patterns are given for phases rather than for the elements. This was done for simplicity of figures and without loss of any information. How to do the recalculation as well theory, apparatus, the experimental procedure and the main rules for interpretation of the DD patterns are given in detail in [2,4,7].

3. Results and discussion

3.1. Inhomogeneity in thin films ZnS·EuS prepared by MO-CVD

A very low Eu solubility in the ZnS lattice is known to result in a phase inhomogeneity if this solubility limit is exceeded. However, the solubility level and origin of precipitates depend crucially on preparation techniques. Here incorporation of EuS in ZnS was studied as a function of partial pressures of volatile Eu and Zn dithiocarbamates during MO-CVD process. At low Eu gas phase pressures the films with overall Eu concentration up to 5 at%, calculated as a ratio Eu/Eu+Zn, are deposited and they all were single-phase according to the X-ray analysis and Raman spectroscopy. Lack of other phases and transformation of undoped cubic ZnS to hexagonal ZnS due to doping was taken as the evidence for the formation of a solid solution in this case [3].

The DD results change radically this concept as seen from Fig. 1. From the shape of kinetic curves and linear profile of the Eu/Zn stoichiogram (Fig. 1a) follows that a single-phase solid solution is indeed formed and identical DD pictures showed all films with overall concentration of Eu below 1 at%. For these films the limiting composition of the solid solution resulted from the Eu/Zn values was found to be $Zn_{0.998}Eu_{0.002}S$. However, all the Eu/Zn line with average values of about 0.007 ± 0.002 reveals two different regions from surface to the depth: the initial one with the value of about 0.025 and the central part as 0.002. This is proof of the inhomogeneous distribution of Eu in the film. The Eu value in depth equal to 0.1 at% was close to that accepted as the equilibrium solubility of Eu in the ZnS lattice. The surface value, equal to 1.25 at% exceeded on the one order that in depth may be interpreted as a pre-precipitate phenomenon.

All the films with overall Eu concentration higher than 1

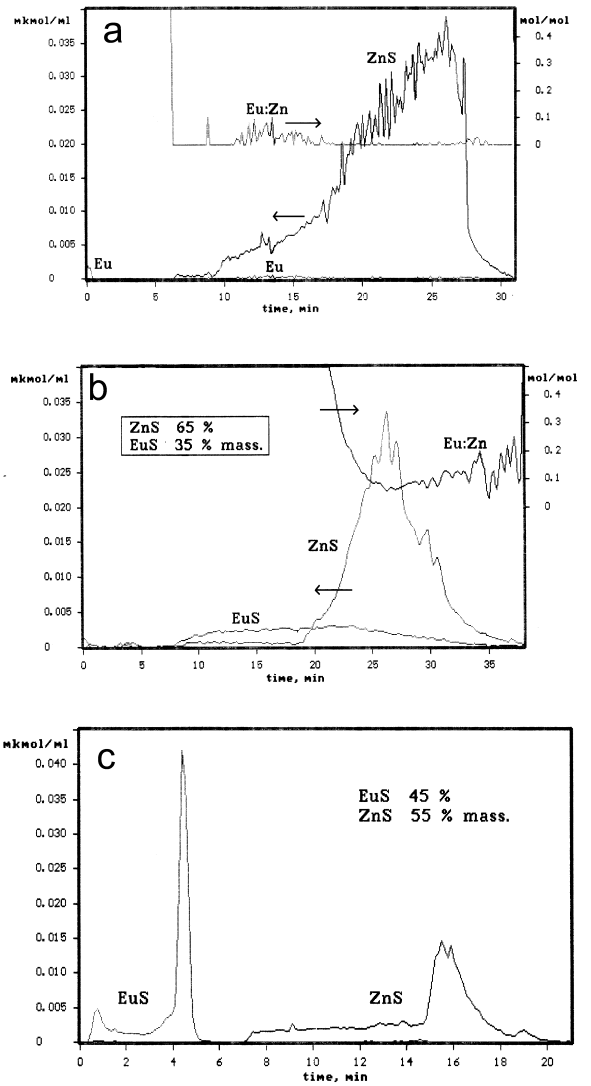

Fig. 1. Profile of kinetic curves of phases dissolving and Eu/Zn stoichiogram for ZnS·EuS films with overall Eu concentration in at% (a) 1.0, (b) 19.5, (c) 57.0. Phases are: (a) $Zn_{0.998}Eu_{0.002}S$; (b) ZnS and $EuS_{amorph.}$; (c) $EuS_{cryst.}$ and $ZnS_{cryst.}$.

at% were heterophased. In the first place intermediates of EuS practically stoichiometric composition appeared, as follows from a variable value of the Eu/Zn line and different than in Fig. 1a the shape of the kinetic curves (Fig. 1b). The shape of kinetic curves itself shows that these intermediates are distributed across the whole film, however, with a increased concentration in surface layers. With the content of about 35% the EuS-intermediates were not observed by the X-ray analysis. Thinking that they are small in the sizes, in parallel with dissolution SEM study was used. For this aim films with the Eu concentration of $\leq$1 and 19% were taken and broken into two parts. Their DD pictures were identical with those given in Fig. 1a,b and their SEM pictures are presented in Fig. 2a,b. Following Fig. 2a, the surface of the film with the low Eu content is smooth and rather uniform without precipitates in ZnS

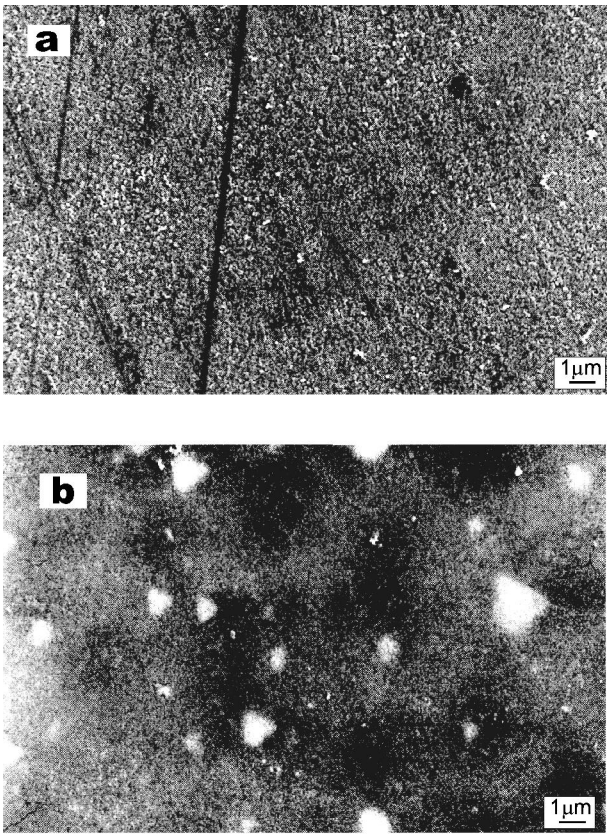

Fig. 2. Scanning electron micrographs of the ZnS·EuS film surface with Eu content in at%: (a) 1, (b) 19.5. The large grains are the EuS clusters covered by organic byproduct.

matrix, that was in line with DD results. The Fig. 2b, like DD, shows precipitates distributed with definite orientation in the ZnS matrix. They look as quite large inclusions of irregular shape. Based on the form, size and the ability of the precipitates to produce an electrical charge under electron beam in SEM study allow us to suggest structure of these inclusions. It was the small in size EuS clusters covered by organic byproducts coming from gas ligand and/or from products of its decomposition.

When the density of the Eu dithiocarbamate flow increases to form films with overall Eu concentration above 40 at%, the stoichiometric EuS phase along with ZnS appeared and they dissolve one after other according to Fig. 1c. This EuS phase is crystalline and thus no problem was to observe also hexagonal EuS phase for these films by the X-ray analysis. A comparison between the pictures in Fig. 1a, b and c shows that at low Eu gas phase pressures during MO-CVD any additional process and unwanted premature reactions could be involved which causes intermediates appearance and inhomogeneities in the film thickness. Today the phenomena of clusters covered by organic byproducts formation during MO-CVD procedure has attracted considerable interest. More details about MO-CVD process with volatile dithiocarbamates of Zn and Eu will be published elsewhere.

3.2. Inhomogeneity of thin films $YBa_2Cu_3O_x$ deposited by laser ablation on sapphire

For these films with thickness of 0.05–0.5 μm DD proved to be very useful in determining the stoichiometry, content of amorphous and impurity phases on micro level, which both are often missed by X-ray techniques. Fig. 3 shows the DD pictures of films $YBa_2Cu_3O_x$ (YBCO) deposited on the substrate at temperatures from 20 to 780°C. While X-ray analysis accomplished nothing for the films deposited at 20–620°C, DD enabled the phase composition to analyze quantitatively. Formation of YBCO, as an amorphous phase, was found to begin at 20°C (Fig. 3a) due to the presence oxide clusters in

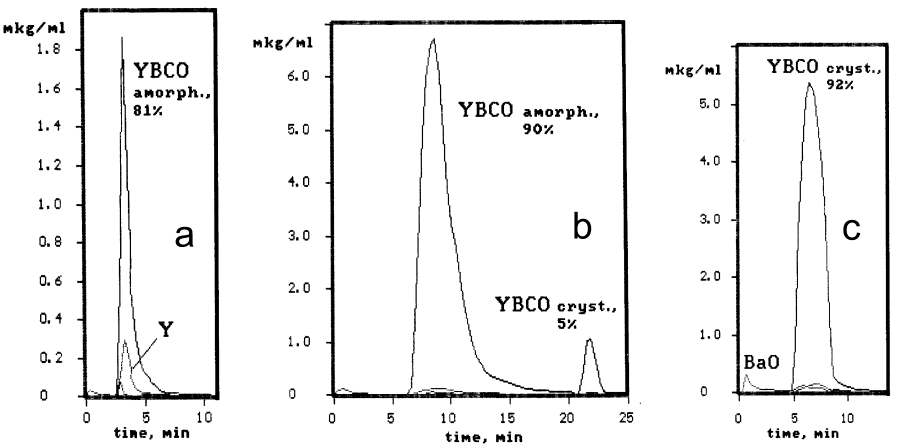

Fig. 3. Profile of kinetic curves of $YBa_2Cu_3O_x$ phase dissolving, films with total weight of 5, 44 and 66 μg deposited on substrate at temperature in °C: (a) 20, (b) 500, (c) 750.

gaseous phase, and amorphous YBCO exists in films down to 500°C (Fig. 3b). Crystalline YBCO begins appear at 500°C and it becomes the only form at 750–780°C (Fig. 3c). Both the amorphous and crystalline YBCO forms were easily identified due to their different ability to dissolve. High-quality and stoichiometric YBCO films have been prepared at 780°C, when any film/substrate interaction was blocked. To realize the scale of this interaction, it will suffice to look at Fig. 4. Minor amount of Al (overall content 0.25%) located near the film–substrate interface was observed, if the film itself was single-crystalline (Fig. 4a). Binary Ba and Cu aluminates distributed in thickness and on surface of the film were observed in the case of a polycrystalline film (Fig. 4b) where overall content of Al was 5.7%. However, in both cases no Al was observed in YBCO phase itself, that is why, having the same value T_C, these films differed by two to three orders in the J_C value. It is significant that the DD results had a dominant role in preparing high quality of YBCO films on sapphire as shown in Ref. [4].

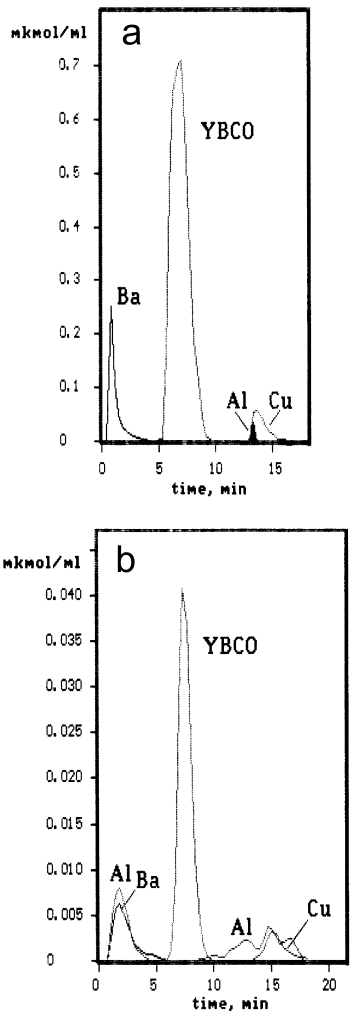

Fig. 4. Kinetic curves of $YBa_2Cu_3O_x$ phase dissolving; films deposited on sapphire at $T_s = 780$°C. (a) Single crystalline state, (b) polycrystalline state.

3.3. Inhomogeneity in crystals $TmBa_2Cu_3O_x$ grown from melt

Doping of $TmBa_2Cu_3O_x$ crystals (Tm123) with CaO is known to influence strongly their superconducting properties by a change of the point defect system. However, introduction into the melt of CaO in a small quantity results in a phase heterogeneity of grown crystals according to the χ–T dependence measured in different magnetic fields (Fig. 5). This heterogeneity could not been explained in a satisfactory manner without detailed structural and chemical study. It does not always happen that Ca enters into the Tm123 lattice. The most widespread anomalies in Tm123 crystals are given in Fig. 6. Variants (Fig. 6a) and (Fig. 6b) show that Ca is not actually incorporated in Tm123 and forms a separate phase, most probably CaO. This phase may be arranged on the crystal surface as seen in Fig. 6a or distributed over the whole thickness of the crystal. In the latter case screening effect for CaO particles appears, and their dissolution goes gradually as follows from the shape of the kinetic curves (Fig. 6b). Doping with Ca did take place but only along with Al and for crystals next to container walls (Fig. 6c). Molar ratio of Ca/Tm123 and Al/Tm123 was found to be identical and equal to about 0.05 in the depth and about 0.5 in the surface layers of the film. Coincident with entering into the lattice, CaO presents here also as a separate phase. So, not only desired Ca dopant, but unwanted Al element may be gettered in the Tm123 crystals. Therefore, reliable interpretation of their superconducting properties is possible if the compositional features of the crystals considered. The local change in stoichiometry of Tm123 observed by DD arises other problem to be solved. This is coexistence of different composition layers and a stacking fault along *c*-axis. To clarify defect structure of these crystals, a structural modeling and special technique of X-ray profile analysis were used that will be published elsewhere.

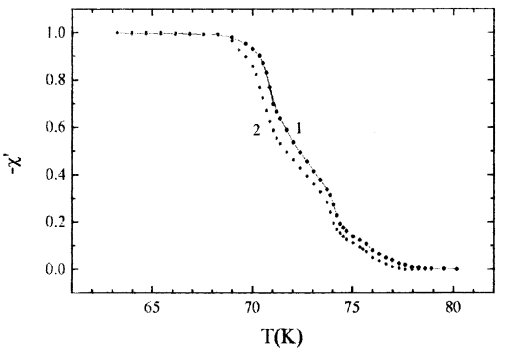

Fig. 5. The χ–T dependence in magnetic field parallel to *ab*-plane of the $TmBa_2Cu_3O_x$ crystal: (1) $H_o = 1.6$ E, (2) $H_o = 5.5$ E.

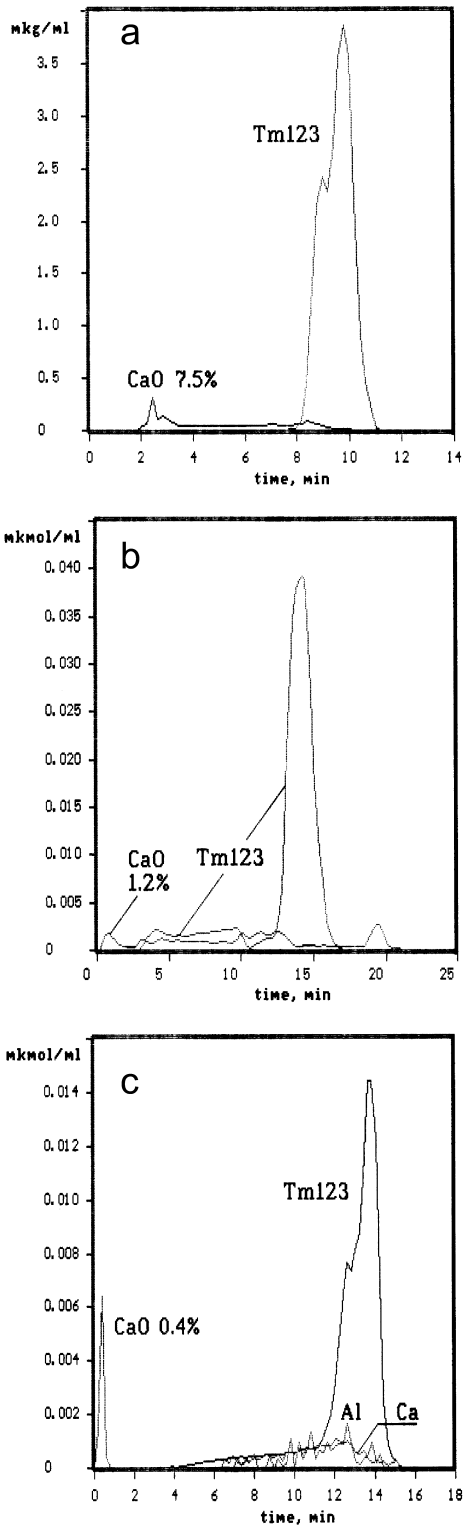

Fig. 6. Profile of kinetic curves of the $TmBa_2Cu_3O_x$ phase dissolving, crystals with overall Ca concentration in mass%: (a) 5.5, (b) 0.93, (c) 1.2.

3.4. Inhomogeneity of powders $Ce_2S_3 \cdot Na_2S$ and $LaFeO_3$ doped with CaO

Accumulation of sodium ions at the powder surface with concentration exceeded the maximum Na/Ce ratio accepted by the cubic structure of γ-Ce_2S_3, as well as a small quantities of impurity polysulfide phases, Na_2S_2 and CeS_2 were established by DD. These features are accompanied the formation of the solid solution γ-$[Na]\cdot Ce_2S_3$ and DD indicates conclusively such state of the powders. This inhomogeneity even on a micro level was shown to result in significant changes of γ-$[Na]\cdot Ce_2S_3$ color characteristics, a new inorganic red pigment [5].

A new information on phase composition of $LaFeO_3$ powder doped with CaO, a catalyst for CO oxidizing, was obtained by DD combined with X-ray analysis. Nano-sized domains of the $Ca_2Fe_2O_5$ composition located on surface of the $LaFeO_3$ powder particles rather than an expected a solid solution $La_{1-x}Ca_xFeO_{3.0-0.5x}$ with $x \leq 0.5$ were found. Boundaries of these microdomains on the powder surface were suggested to be active centers responsible for catalytic properties of this material. Other experimental details about this catalyst may be found in Ref. [6].

4. Conclusions

In summary, we developed a new technique which allows the chemical inhomogeneity to be controlled precisely and reliably. The examples given here demonstrate that it is possible to identify different kinds of inhomogeneity even for materials in a small quantity. In each case in these studies, conditions were established under which optimized materials have been prepared. This has motivated further application of DD to characterize other materials.

Acknowledgements

This work was supported by the Russian Foundation of Fundamental Research, grant 00-03-32516.

References

[1] S. Hofmann, in: D. Briggs, M.P. Seah (Eds.), Practical Surface Analysis by Auger and X-ray Photoelectron Spectroscopy, Wiley, Chichester, 1985, p. 141.
[2] V. Malakhov, Zh. Anal. Khim. 44 (1989) 1177–1190.
[3] V. Bessergenev, E. Ivanova, Yu. Kovalevskaya, I. Vasilyeva et al., Mater. Res. Bull. 32 (1997) 1403–1410.
[4] I. Vasilyeva, V. Malakhov, A. Vlasov, M. Predtechensky, Thin Solid Films 292 (1997) 85–90.
[5] I. Vasilyeva, B. Ayupov, A. Vlasov, V. Malakhov, P. Macaudiére, P. Maestro, J. Alloys Comp. 268 (1998) 72–77.
[6] L. Isupova, I. Yakovleva, S. Zibulya et al., Kinetika i Katalis 41 (2000) 315–320, in Russian.
[7] V. Malakhov, A. Vlasov, Kinetika i Katalis 36 (1995) 503–515, in Russian.